ORIGINAL ARTICLE

ORAL DISEASES WILEY

Targeting TGF beta receptor 1 in head and neck squamous cell carcinoma

Bernhard J. Jank[1] | Julia Schnoell[1] | Katharina Kladnik[1] | Carmen Sparr[1] |
Markus Haas[1] | Elisabeth Gurnhofer[2] | Alexander L. Lein[1] | Markus Brunner[1] |
Lukas Kenner[2,3,4,5] | Lorenz Kadletz-Wanke[1] | Gregor Heiduschka[1]

[1]Department of Otorhinolaryngology, Head and Neck Surgery, Medical University of Vienna, Vienna, Austria

[2]Department of Experimental Pathology and Laboratory Animal Pathology Department of Pathology, Medical University of Vienna, Vienna, Austria

[3]Unit of Laboratory Animal Pathology, University of Veterinary Medicine, Vienna, Austria

[4]Christian Doppler Laboratory for Applied Metabolomics, Vienna, Austria

[5]CBmed GmbH – Center for Biomarker Research in Medicine, Graz, Austria

Correspondence
Bernhard J. Jank, Department of Otorhinolaryngology, Head and Neck Surgery, Medical University of Vienna, Währinger Gürtel 18-20, 1090 Vienna, Austria.
Email: bernhard.jank@meduniwien.ac.at

Funding information
City of Vienna Fund for Innovative Interdisciplinary Cancer Research

Abstract

Objectives: The transforming growth factor-Beta (TGF-ß) pathway may be involved in the radioresistance of head and neck squamous cell carcinoma (HNSCC). This study analyzed TGF-ß receptor 1 (TGFBR1) expression in HNSCC patients and evaluated the antineoplastic and radiosensitizing effects of vactosertib, a novel TGFBR1 inhibitor, in vitro.

Materials and Methods: TGFBR1 expression was examined in HNSCC patients at the mRNA level in silico and the protein level by immunohistochemistry, including surgical specimens of primary tumors, matched lymph node metastasis, and recurrent disease. Furthermore, a novel small molecule TGFBR1 inhibitor was evaluated in HNSCC cell lines. Finally, an indirect coculture model using patient-derived cancer-associated fibroblasts was applied to mimic the tumor microenvironment.

Results: Patients with high TGFBR1 mRNA levels showed significantly worse overall survival in silico (OS, $p = 0.024$). At the protein level, an association between TGFBR1^{+} tumor and OS was observed for the subgroup with TGFBR1-stroma ($p = 0.001$). Those results prevailed in multivariable analysis. Inhibition of TGFBR1 showed antineoplastic effects in vitro. In combination with radiation, vactosertib showed synergistic effects.

Conclusion: Our results indicate a high risk of death in $tumor^{TGFBR1+}|stroma^{TGFBR1-}$ expressing patients. In vitro data suggest a potential radiosensitizing effect of TGFBR1 inhibition by vactosertib.

KEYWORDS
cancer-associated fibroblasts, head and neck cancer, radiosensitizer, TGF ß, TGF ß receptor 1, vactosertib

---

Bernhard J. Jank and Julia Schnoell contributed equally to this work.

1 | INTRODUCTION

Head and neck squamous cell carcinomas are among the 10 most common cancers worldwide (Johnson et al., 2020; Sung et al., 2021). While most HPV$^+$ oropharyngeal HNSCC patients show a good prognosis due to high radiosensitivity, survival rates of HPV$^-$ patients are still dismal (Chaturvedi et al., 2011; Johnson et al., 2020). In those patients, radioresistance is a major obstacle to curative treatment (Perri et al., 2015). To date, the only approved radiosensitizers are cisplatin, a chemotherapeutic agent, and cetuximab, a monoclonal antibody targeting the epidermal growth factor receptor (EGFR; Yamamoto et al., 2016). Mechanisms behind radioresistance involve many pathways, amongst them the transforming growth factor-beta (TGF-β) pathway (Centurione & Aiello, 2016). TGF-β signaling is essential for epithelial tissue homeostasis and exerts tumor-suppressing properties (Tian & Schiemann, 2009). However, once carcinogenesis is initiated, the TGF-ß pathway often becomes aberrated and can switch to tumor-promoting effects like promotion of invasion, migration, and immune evasion (Sheen et al., 2013; Teicher, 2021). TGF-β expression is enhanced in most HNSCC patients and an association with a worse outcome has been shown (White et al., 2010). Furthermore, radiation treatment induces the expression of TGF-β, rendering it a potentially interesting target for radiosensitization (Centurione & Aiello, 2016). Essential sources of TGF-β are autocrine signaling and the tumor microenvironment, mainly consisting of cancer-associated fibroblasts (CAFs). CAFs have been shown to promote proliferation, invasion, metastasis, and drug resistance (Peltanova et al., 2019). TGF-β-targeted therapies have already shown favorable results, which reduce the tumor-promoting effects associated with CAFs and radioresistance in different cancer entities (Bouquet et al., 2011; Erdogan & Webb, 2017; Yu et al., 2014).

There is an unmet need for a potent radiosensitizer in the treatment of HNSCC patients, and the TGF-ß receptor 1 (TGFBR1) might be a promising target. Vactosertib (TEW7197, EW-7197) is an orally available small molecule inhibitor of TGFBR1. Early studies have shown encouraging antineoplastic effects in breast cancer (Song et al., 2019), lung cancer (Kaowinn et al., 2017), and melanoma models (Yoon et al., 2013). Vactosertib is currently under investigation in clinical phase I and II studies for solid tumors (Jung, Yug, et al., 2020; Wang et al., 2020). However, there is no data on the effect of vactosertib in HNSCC. Therefore, this study aimed to investigate the relationship between the expression of TGFBR1 and disease outcomes in HNSCC and to evaluate the antineoplastic and radiosensitizing effect of vactosertib in HNSCC in vitro.

2 | MATERIALS AND METHODS

2.1 | Patient population

Two independent datasets were used for our analysis. First, for the analysis of TGFBR1 at the mRNA level, a dataset was extracted from The Cancer Genome Atlas (Firehose Legacy, TCGA) via cBioportal.org in February 2022 (Cerami et al., 2012; Gao et al., 2013). From 530 patients included in this dataset, we manually excluded all patients with incomplete TNM-staging, missing mRNA data for TGFBR1, and overall survival (OS) of fewer than 2 months. Four hundred and eighty-nine patients could be included in the analysis. High-TGFBR1 mRNA levels were defined as an mRNA z-score above 2, relative to diploid samples. Second, to analyze TGFBR1 at the protein level, we used the tumor microarray (TMA) of our in-house HNSCC study population. This cohort includes 130 patients with histologically diagnosed squamous cell carcinoma of the head and neck. The cohort was homogenously treated at the Vienna General Hospital with surgical resection with curative intent, followed by postoperative radiotherapy between 2002 and 2012. The last follow-up of this cohort occurred in September 2018. Exclusion criteria were the following: external treatment, secondary primary carcinoma, distant metastasis (M1), prior radiation, or immunosuppression. HPV was assessed using in situ hybridization. Data were collected retrospectively from the electronic patient record system of the Vienna General Hospital. The eighth edition AJCC manual was used for staging of tumors of both datasets. This study was approved by the ethics committee of the Medical University of Vienna, EK 1311/2018.

2.2 | Tissue microarray and immunohistochemistry

TMAs were constructed as described previously (Jank et al., 2021). Briefly, three 1000 μm cores per patient sample of surgically resected tumor tissue were generated. For staining, specimens were cut in 2.5–μm-thick sections, deparaffinized and rehydrated following standard protocols. After antigen retrieval and endogenous peroxidase activity block, the primary antibody (Anti-TGF beta Receptor I, ab235178, Abcam) was applied for 1 h at room temperature. Then, a primary antibody enhancer was applied for 10 min, and horseradish peroxidase polymer was applied for 15 min. Visualization was achieved by UltraVision Plus Detection System DAB Plus Substrate System (Thermo Scientific). Counterstaining was performed with hematoxylin Gill III (Merck). Staining was categorized into negative (−) (<10% of cells with weak staining), "weak" (+) positive (>10% of cells with weak staining), or "strong" (++) positive (>10% of cells with strong staining). Images were taken on an inverted microscope (Olympus IX73, Olympus Corp.).

2.3 | Cells and reagents

The two HPV-HNSCC cell lines, FaDu and SCC25, were obtained from American Type Culture Collection (ATCC). The HPV$^+$ HNSCC cell line SCC154 was purchased from the German Collection of Microorganisms and Cell Cultures (Leibnitz). All cell lines were cultured in Dulbecco's Modified Eagle's Medium (DMEM; Thermo Fisher) supplemented with 10% fetal bovine serum (Life Technologies) and 100 U/mL penicillin, 100 μg/mL streptomycin (Thermo Fisher) in a humidified atmosphere at 37°C with 5% CO_2. Cells were used for experiments up to passage 30.

Vactosertib (EW7197) was purchased from Selleck Chemicals, dissolved in DMSO (Thermo Fisher), and stored as a stock solution at −80°C following the manufacturer's instructions. After thawing, the aliquots were stored at 4°C for up to 30 days. The final concentration of DMSO in the cell culture medium was kept below 0.15%. Resazurin Sodium Salt (Sigma-Aldrich) was stored after sterile filtration as a 10× stock solution of 560 μM dissolved in PBS protected from light at 4°C.

2.4 | Irradiation

Radiation was carried out using a 200 kV YXLON Maxishot X-ray unit (YXLON International GmbH). Cells were irradiated at room temperature with 2, 4, 6, or 8 Gy. The applied dose was 1 Gy/min at a fixed-focus object distance of 45.5 cm. The acceleration voltage was 200 kV at a current of 20 mA with a focus size of 5.5 mm using a 4 mm Al and 0.6 mm Cu filter. Experiments were analyzed 72 h after radiation exposure.

2.5 | Isolation of CAFs

Cancer-associated fibroblasts were extracted from biopsies of fresh human HNSCC samples of patients treated at the Medical University of Vienna. The protocol was approved by the ethics committee of the Medical University of Vienna (ECS no. 2313/2019) and informed consent was obtained from all human subjects. Inclusion criteria for patients were the histopathological diagnosis of an HNSCC tumor greater than T2 and a patient aged between 18 and 80 years old. Exclusion criteria were previous cancer treatment and immunosuppression. During surgery, a small piece of approximately 5 mm³ was biopsied from the resected tumor specimen and immediately stored in an ice-cold culture medium supplemented with 1000 U/mL penicillin, 1000 μg/mL streptomycin, and 2.5 μg/mL amphotericin B (Sigma-Aldrich).

Subsequently, the tissue was washed twice with PBS and cut into smaller pieces of approximately 1–3 mm³ using sterile scalpels. The samples were then transferred to a dry Petri Dish and incubated with 1–2 drops of TrypLE Express Enzyme (Thermo Fisher) for 15 min at 37°C. Subsequently, 5–7 pieces were transferred into one well of a 6-well plate and covered with minimal amounts of primary culture medium (DMEM +100 U/mL penicillin, 100 μg/mL streptomycin, 100 μg/mL gentamycin; Thermo Fisher), and 0.25 μg/mL amphotericin B at room temperature for 15 min to ensure attachment of the tissue samples to the culture dish. Samples were then incubated in the primary culture medium for 1 day. After 24 h of incubation, the wells were carefully filled with another 1 mL of primary culture medium. The primary culture medium was replaced by standard medium after 2 days of incubation. CAFs started to grow out of the tumor tissue within 2 weeks of incubation. Subculturing was performed after CAFs covered approximately 80% of the culture dish. Wells were washed with PBS, treated with 0.3 mL of 0.05% Trypsin-0.53 mM

EDTA, and incubated for 5–20 min. Fibroblasts detached faster than other cells and thus could be filtered out and transferred to another culture dish for further cultivation. A visual control under the microscope confirmed that only fibroblasts formed a morphologically homogenous subculture. The subcultured CAFs were used for experiments until passage 9.

2.6 | Immunocytochemistry of CAFs

Immunofluorescent staining of the CAF-specific markers alpha-smooth muscle actin (α-SMA, 1:250, Abcam, ab124964) and fibroblast activation protein (FAP, 1:500, Abcam, ab53066) was performed to ensure CAF phenotype following standard protocols. Additionally, cells were stained with Pan-Cytokeratin (pCK, 1:50, Sigma Aldrich, C2562) to confirm the absence of epithelial cells. HaCat (Thermo Fisher) cells served as a positive control for Pan-Cytokeratin staining.

2.7 | CAF conditioned medium

Isolated CAFs were cultured in a Petri dish until they reached approximately 70% confluency. Subsequently, the medium was replaced by a fresh culture medium, and the conditioned medium was harvested after 48 h of incubation. Debris was removed by centrifugation at 1200 rpm for 10 min. The conditioned medium was stored at −20°C for long-term storage. CAF CM of the same donor was pooled for experiments and stored for up to 30 days at 4°C. CM was mixed with fresh culture medium (1:1) for use in experiments to ensure sufficient nutrient supply.

2.8 | Metabolic activity assay

FaDu and SCC25 cells (5×10^3) and SCC154 cells (10×10^3) were seeded per well in 96-well plates. Cells were incubated for 24 h before treatment. DMSO (0.1%) was used as control. Metabolic activity was assessed after 72 h incubation using a colorimetric resazurin-based assay. In brief, cells were incubated in 56 μM resazurin sodium salt (Sigma-Aldrich) diluted in the standard culture medium for 60 min. Subsequently, measurements were taken at an excitation wavelength of 570 nm and an emission wavelength of 600 nm using a microplate reader (Tecan Spark®, Tecan Group Ltd.). Measurements were normalized to blank readings.

2.9 | Migration assay

Migration was assessed using a cell exclusion assay (FaDu, SCC25) or a scratch assay (SCC154). Twenty-four hours after cell seeding, the 2-well Ibidi silicone inserts (Ibidi) were removed, or a scratch was performed using a 10 μL pipette tip. Cell migration was assessed 24 h

after treatment. The effect of CAF conditioned medium on migration was analyzed similarly. CAF CM#1 was used for all subsequent analyses because it showed the most significant effect in the proliferation assay. To assess cell migration, pictures of the gap were taken at 0h and 24h. The gap closure was evaluated using ImageJ ("MRI Wound Healing Tool"). The gap area was normalized to the vehicle control.

2.10 | Colony formation assay

The clonogenic potential was assessed using a colony formation assay as described previously (Franken et al., 2006). In brief, cells were seeded in 6-well plates at increasing densities to compensate for the effect of higher radiation doses. Vactosertib was added to the culture medium for 72h. After that, the medium was changed to a drug-free medium. Since SCC154 cells would not form colonies in the standard culture medium, they were incubated with a conditioned medium from irradiated human dermal fibroblasts (HDFn, ATCC, Manassas, VA, USA). Subsequently, the cells were scanned using brightfield imaging on a TECAN multimode microplate reader (Tecan Spark®, Tecan Group Ltd.). Colonies were automatically counted using ImageJ.

2.11 | Trypan blue exclusion assay

FaDu, SCC25, and SCC154 cells were seeded in 12-well plates and incubated for 24h. Subsequently, the cells were treated with vactosertib radiation and incubated for 72h. After incubation, the medium containing dead cells was collected by aspiration, and attached cells were collected by trypsinization. Cells were then pelleted at 500g for 5min, resuspended, and mixed with trypan blue (1:1; Sigma-Aldrich). The percentage of dead cells was counted according to their size, shape, and trypan blue uptake, using the Countess FL Automated Cell Counter (Thermo Fisher). Results were normalized to the untreated control group of each cell line and reported as percentages.

2.12 | Statistical analysis

Survival analysis was performed using Stata/IC (Macintosh version 16.1, Stata Corp). Disease-free survival (DFS) was defined as the time from surgery to the histologically confirmed recurrence or death of any cause in patients without recurrence. OS was defined as the time from surgery to the time of death from any cause. OS and DFS were estimated using the Kaplan–Meier estimator. For survival analysis, mRNA levels were dichotomized into high (z-score >2) or low (z-score ≤2) and protein expression was dichotomized into positive (weak and strong staining) and negative. Log-rank tests were used to compare groups, and uni- and multivariable Cox proportional hazard models were used for modeling. All multivariable models were

adjusted for TNM stage, smoker status, and HPV status. Pairwise interaction terms between TGFBR1 expression in tumor cells and the stroma of primary tumors were added to evaluate differences in the association with outcomes. Hazard ratios (HR) and 95%CI were calculated. A two-sided $p < 0.05$ was considered statistically significant. Statistical analysis of in vitro experiments was performed using GraphPad Prism for Mac Version 8 (GraphPad Software, LLC.). Dose–response curves and IC_{50} values were calculated by applying nonlinear regression fitting to a variable slope model. Statistical significance of differences between groups was calculated using a two-way analysis of variance (ANOVA), followed by post hoc testing using Tukey's correction for multiple comparisons. All results represent the mean±SD of at least three independent replicates. Interaction analysis of combination treatment for vactosertib with radiation was performed using the SynergyFinder web application (version 3.0; https://synergyfinder.fimm.fi; Ianevski et al., 2020). Synergy scores were calculated according to the zero-interaction potency (ZIP) model, with ZIP scores >10 representing synergistic, 10 to −10 representing additive, and <−10 representing antagonistic drug-radiation interactions.

3 | RESULTS

3.1 | TGFBR1 expression is associated with worse survival

To determine an association of TGFBR1 with disease outcomes in HNSCC patients, we first performed an in silico survival analysis using The Cancer Genome Atlas dataset. The baseline characteristics of the dataset used in this study are summarized in Table 1. During a median follow-up of 2.86years (Q1-Q3; 1.75–4.71), a total of 211 (43%) patients died, and 139 (38%) suffered from disease recurrence. To analyze whether TGFBR1 mRNA levels influenced disease outcomes, we dichotomized patients into high or low mRNA levels at a z-score of +2. Of the 489 patients included in the analysis, 368 (75%) were classified as "high." Kaplan–Meier estimators and the log-rank test revealed an association between high TGFBR1 mRNA levels and worse 5-year overall survival (61% vs. 44%, $p = 0.024$, Figure 1a). No differences in DFS were found (5-year DFS: 54% vs. 49%, $p = 0.484$, Figure S1A). Subsequently, uni- and multivariable Cox regression models were calculated to correct for possible confounders. The univariable model calculated a 50% increased risk for death for patients with high TGFBR1 mRNA levels. This result prevailed after correction for potential confounders (HR 1.652, 95%CI 1.10–2.48, $p = 0.016$, corrected for HPV status, TNM stage, and smoker status). Next, we analyzed if TGFBR1 mRNA levels were associated with clinicopathological characteristics. We found an association with HPV status. HPV⁻ patients were more likely to have high TGFBR1 mRNA levels than HPV⁺ patients (78% vs. 63%, $p = 0.010$, Table S2).

To validate this finding at the protein level, we investigated immunohistochemical staining for TGFBR1 in TMAs of our in-house

TABLE 1 Baseline characteristics of both cohorts.

	TCGA (*n* = 489)	TMA (*n* = 113)
Gender		
Female	128 (26%)	26 (23%)
Male	361 (74%)	87 (77%)
Age at diagnosis (Q1–Q3)	61 (53–69)	59 (53–63)
T-stage	*n* = 475	
T1	32 (7%)	23 (20%)
T2	140 (29%)	58 (51%)
T3	127 (27%)	20 (18%)
T4	176 (37%)	12 (11%)
N-stage	*n* = 468	
N0	224 (52%)	22 (25%)
N1-3	205 (48%)	67 (75%)
N0 (HPV$^+$ OPX)	9 (23%)	2 (8%)
N1-3 (HPV$^+$ OPX)	30 (77%)	22 (92%)
TNM-staging	*n* = 475	
I-II	128 (27%)	38 (34%)
III-IV	348 (73%)	75 (66%)
HPV	*n* = 447	*n* = 111
+	62 (14%)	24 (22%)
−	385 (86%)	87 (78%)
Primum		
Oral cavity	300 (61%)	30 (27%)
Oropharynx	70 (14%)	51 (45%)
Larynx	109 (2%)	12 (11%)
Hypopharynx	10 (2%)	20 (18%)
Alcohol use	NA	*n* = 98
Nondrinker		60 (61%)
Active drinker		38 (39%)
Smoking status	*n* = 477	*n* = 112
Non/Ex-smoker	311 (65%)	34 (31%)
Smoker	166 (35%)	78 (69%)
Marker expression mRNA		
TGFBR1 high	368 (75%)	−
Marker expression IHC		
TGFBR1 TU		
Negative	−	17 (15%)
Weak	−	71 (63%)
Strong	−	25 (22%)
TGFBR1 STRO		
Negative	−	15 (13%)
Weak	−	78 (69%)
Strong	−	20 (18%)

HNSCC cohort. We utilized primary tumor samples (*n* = 113), matched samples of lymph node metastasis (*n* = 38), and samples of recurrent disease (*n* = 16). Tumor cells and stromal cells were categorized separately for TGFBR1 protein expression. All possible combinations of staining intensities between tumor and stroma were observed (Figure 2a).

The median follow-up time of our in-house (TMA) cohort was 9.3 years (Q1–Q3; 5.9–11.8), during which we observed 40 recurrences (35%) and 58 deaths (51%). All patients received postoperative radiotherapy ranging from 40 to 70 Gy. Further baseline characteristics of the TMA cohort are summarized in Table 1. Of the 113 primary tumors, 11% (*n* = 12) were double-negative for TGFBR1 (tumor cells and stroma), while 12% (*n* = 14) were double-strong positive, and the majority stained double weak positive (57%). In lymph node metastasis, 3% (*n* = 1) were double negative, and 8% (*n* = 3) were double strong positive, with the majority being double-weak positive (35%). In recurrent disease, 25% (*n* = 4) were double negative, and none were double positive (Figure 2A,B). With disease progression, we observed an increase in negative staining of the tumor stroma from 13% in primary tumor samples to 44% in samples of recurrent disease. This trend was also observed in the staining of tumor cells (15% increased to 31%). However, this difference was not significant (*p* = 0.089 and 0.082, respectively; Figure 2C).

To determine whether TGFBR1 expression played any role in disease outcomes, we performed a survival analysis examining OS and DFS. For survival analysis, protein expression was dichotomized into positive (weak and strong staining) and negative. Kaplan–Meier estimators and log-rank test revealed no differences for TGFBR1 protein expression of the primary tumor and OS (tumor staining *p* = 0.549; stromal staining *p* = 0.863; Figure 1B top row) or DFS (tumor staining *p* = 0.397; stromal staining *p* = 0.252, Figure S1B top row). Uni- and multivariable Cox analysis corroborated this result (Table 2 and Table S1). Next, we analyzed the effect of TGFBR1 protein expression in samples of matched lymph node metastasis (*n* = 38) on OS and DFS. We found a significant association between TGFBR1 protein expression of tumor cells in lymph node metastasis and a worse OS (5-year OS: neg.: 100%; pos.: 49%; *p* = 0.031, Figure 1b middle row). This result prevailed in a multivariable cox regression analysis after correction for possible confounders (TGFBR1 tumor pos. vs. neg.: HR: 16.110; 95% CI: 1.15–225.21, *p* = 0.039).

Interestingly, the TGFBR1 expression of stromal cells in lymph node metastasis showed an inverse association with OS (5-year OS, TGFBR1 neg.: 24%, pos.: 68%, *p* < 0.000, Figure 1b middle row). This result also prevailed in multivariable analysis (TGFBR1 stroma pos. vs. neg. HR: 0.148; 95% CI: 0.04–0.46, *p* = 0.001). No difference was found for DFS (Figure S1B and Table S1).

Finally, we analyzed matched samples of recurrent disease (*n* = 16) for TGFBR1 expression and its association with OS. No association with OS could be found (tumor: *p* = 0.160; stroma: 0.951, Figure 1b bottom row, Table 2).

Based on the observation that stromal TGFBR1 expression in lymph node metastasis was inversely correlated with disease outcome, we hypothesized that stromal TGFBR1 expression might exert tumoristatic effects (i.e., halting tumor progression). Subsequently, we performed a subgroup analysis for the association of TGFBR1 tumor cell expression with disease outcomes in patients with
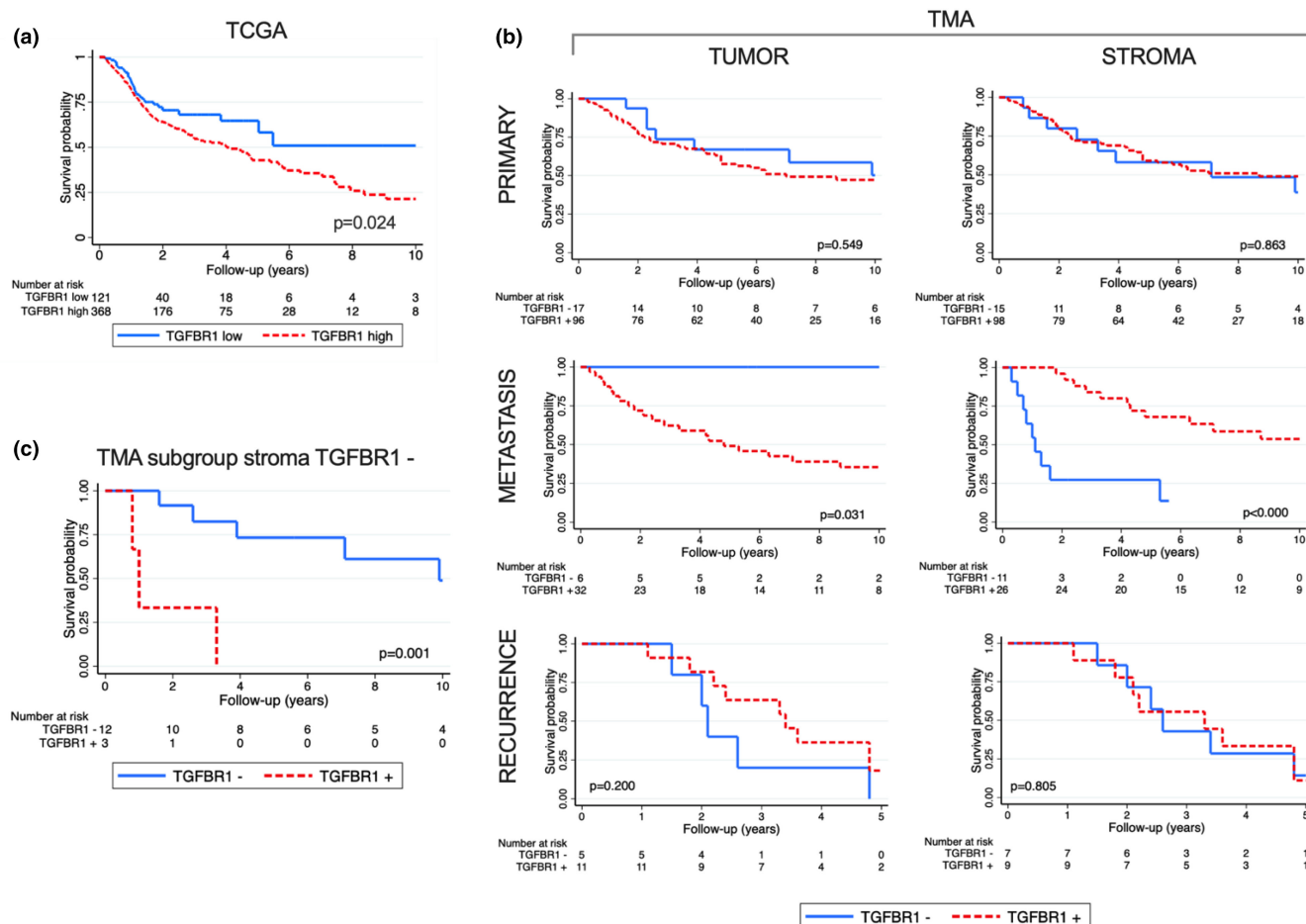
FIGURE 1 Kaplan–Meier estimators for OS according to TGFRB1 expression. (a) Kaplan–Meier estimator showing the influence of TGFBR1 mRNA levels on OS in a dataset of The Cancer Genome Atlas. (b) Kaplan–Meier estimators for OS and TGFBR1 protein expression in primary HNSCC samples (top row), matched samples of lymph node metastasis (middle row), and samples of recurrent disease (bottom row) of a secondary dataset. (c) Kaplan–Meier estimator for subgroup analysis of patients with negative stromal staining for the effect of tumor cell TGFBR1 expression of primary tumor samples.

TGFBR1- stroma. In this subgroup, TGFBR1 tumor cell expression showed a significant association with OS (5-year OS pos.: 0%; neg.: 73%, $p=0.001$, Figure 1c). Univariable cox models including a pairwise interaction of TGFBR1 expression in tumor cells with TGFBR1 expression in the stroma showed statistically significant evidence for an interaction (TGFBR1 stro⁻ HR: 9.055; 95%CI: 2.09–39.11; $p=0.003$; TGFBR1 stro⁺ HR:1.394; 95%CI: 0.55–3.51; $p=0.480$). This result prevailed in multivariable analysis (TGFBR1 stro⁻ HR: 4.799; 95%CI: 1.03–22.27; $p=0.045$; TGFBR1 stro⁺ HR: 0.955; 95%CI: 0.35–2.56; $p=0.927$; Table 2).

Finally, we analyzed for associations of marker expression with clinicopathological patient characteristics. In the TMA cohort, we found TGFBR1 protein expression in tumor cells of primary tumors to be associated with lymph node status and HPV status. Patients without lymph node metastasis showed a higher proportion of tumors with strong TGFBR1 expression (50% vs. 15%; $p<0.001$), and HPV⁻ patients also had a higher rate of tumors with strong TGFBR1 expression (26% vs. 4%; $p=0.001$, Table S4).

3.2 | In vitro effects of a small molecule TGFBR1 inhibitor on HNSCC

First, we determined the effect of vactosertib on the metabolic activity of three HNSCC cell lines (two HPV⁻ [FaDu and SCC25], one HPV⁺ [SCC154]) using a resazurin reduction assay. Vactosertib treatment decreased metabolic activity dose-dependently with IC$_{50}$ values ranging between 35 and 66μM, with SCC25 being the most sensitive cell line (Figure 3a).

3.3 | Vactosertib shows synergistic effects in combination with radiation

Next, we aimed to determine the radiosensitizing effect of vactosertib. Cell lines were exposed to increasing concentrations of vactosertib in combination with radiation, and the metabolic activity was measured as described above. The combination of
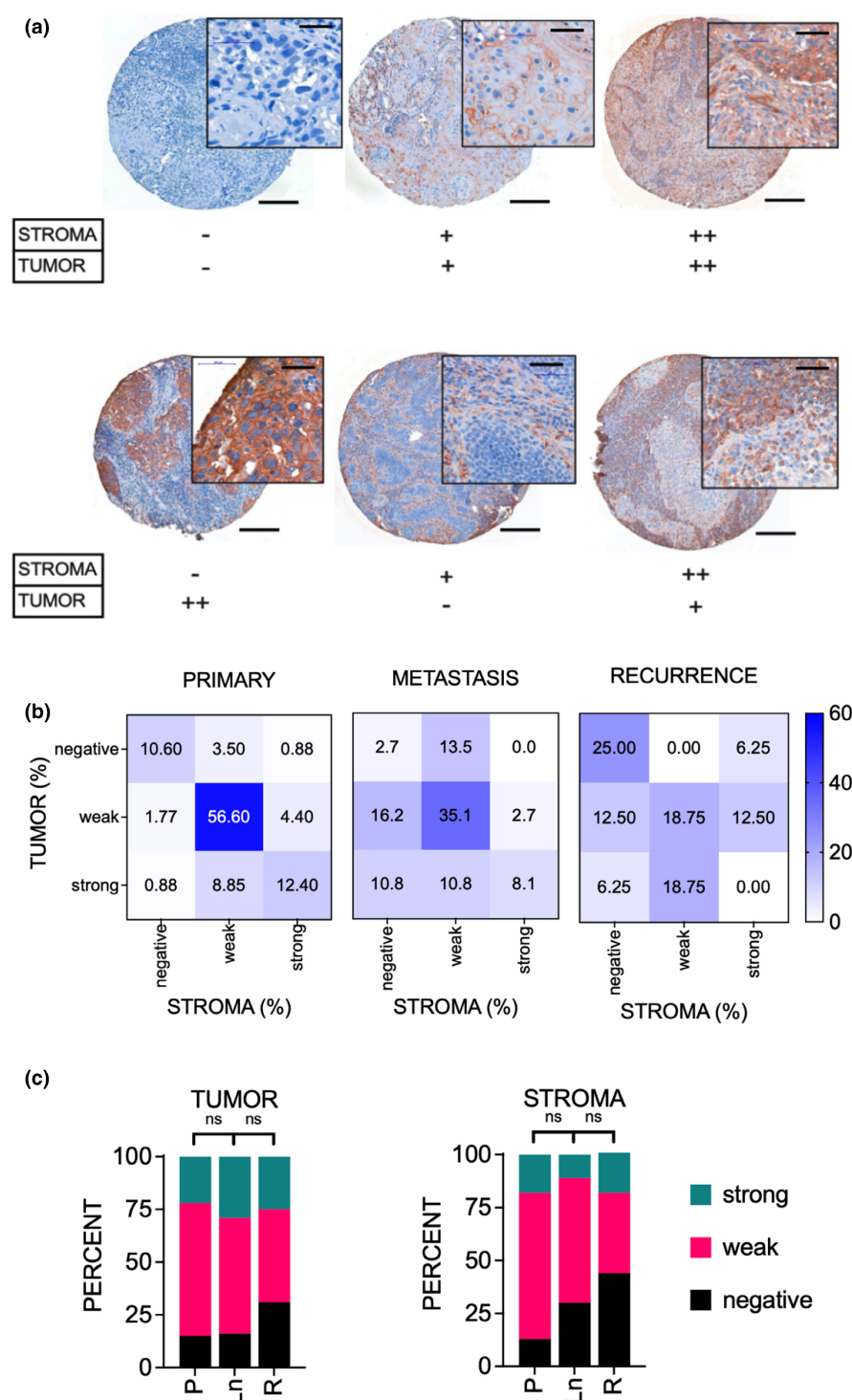
FIGURE 2 TGFBR1 expression patterns during disease progression. (a) Representative images of IHC staining for TGFBR1 of TMA samples with a selection of different expression patterns between tumor and stromal cells. Scale bars, TMA 200 μm; insets 50 μm. (b) Heatmap visualization of staining patterns observed during disease progression, left in primary tumor samples (n = 113), middle in matched lymph node metastasis (n = 38), and right in recurrent disease samples (n = 16). (c) Changes in TGFBR1 expression at different stages of disease separated for tumor cells (left) and stromal cells (right; P = primary tumor; Ln = lymph node metastasis; and R = recurrent disease).

vactosertib and radiation significantly reduced metabolic activity in all tested cell lines. The inhibitory effect at 2 Gy was strongest in SCC25 (ctrl.: 90% ± 8.3% vs. 75 μm: 19% ± 8.9%, $p < 0.001$), followed by Fadu (90% ± 5.8% vs. 27% ± 8.7%, $p < 0.001$) and SCC154 (81% ± 13.8% vs. 39% ± 9.5%, $p < 0.001$; Figure 1b). To determine the combinatory effect, Synergy maps were calculated using the Synergyfinder tool (https://synergyfinder.fimm.fi/). The overall synergy score was highest for FaDu (14.3 ± 5.1), followed by SCC25 (12.4 ± 6.9) and SCC154 (3.7 ± 9.1). In detail, FaDu and

SCC25 showed synergistic and additive effects for all combinations. SCC154 mostly showed additive effects, but a synergistic effect was observed for the combination of 25 μM vactosertib with radiation doses of 2 and 8 Gy (Figure 3c).

To determine the cytotoxic effect of vactosertib, we performed a trypan blue exclusion assay. SCC25 was the only cell line with increased cell death compared to the control group in a single treatment (ctrl.: 0% ± 10% vs. 75 μm: 13% ± 7.6%; $p = 0.019$, Figure 3d middle). FaDu showed increased cell death in combination with radiation

TABLE 2 Uni- and multivariable Cox regression for OS in TCGA and TMA datasets.

	Univariable			Multivariable		
	HR	95% CI	*p*-Value	HR	95% CI	*p*-Value
TCGA						
TGFBR1 high versus low	1.513	1.05–2.17	0.026	1.652	1.10–2.48	0.016
TMA						
PRIMARY						
TGFBR1 tu:	1.254	0.59–2.65	0.553	0.882	0.39–1.98	0.762
TGFBR1 stro:	0.936	0.44–1.97	0.864	0.651	0.29–1.44	0.292
TGFBR1 tu+.:						
TGFBR1 stro+	1.394	0.55–3.51	0.480	0.955	0.35–2.56	0.927
TGFBR1 stro−	9.055	2.09–39.11	0.003	4.799	1.03–22.27	0.045
METASTASIS						
TGFBR1 tu (*n* = 38)	7.210	0.92–55.92	0.059	16.110	1.15–225.21	0.039
TGFBR1 stro (*n* = 37)	0.145	0.05–0.39	<0.000	0.148	0.04–0.46	0.001
RECURRENCE						
TGFBR1 tu (*n* = 16)	0.508	0.16–1.54	0.233	0.153	0.0–0.87	0.035
TGFBR1 stro (*n* = 16)	1.131	0.40–3.19	0.815	1.287	0.31–5.21	0.724

Note: Multivariable models were adjusted for TNM-stage, HPV status, and smoker status.
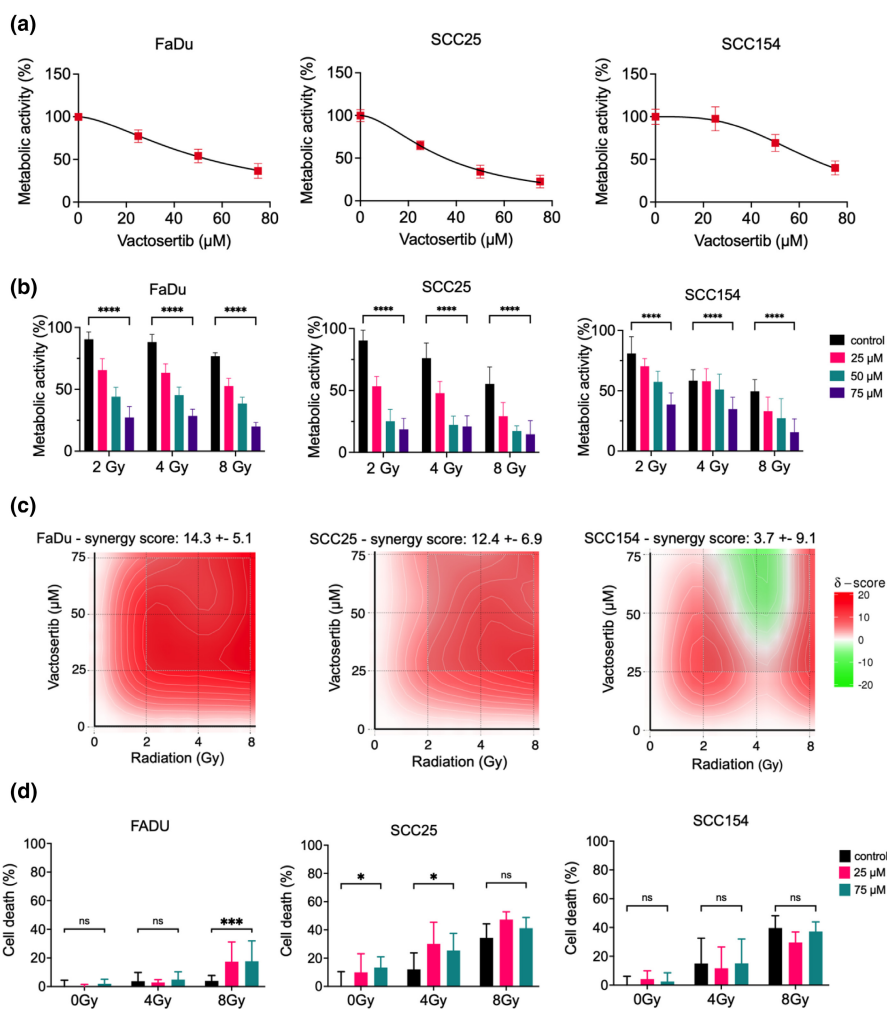
FIGURE 3 Effect of TGFBR1 inhibition on metabolic activity and cell viability in three HNSCC cell lines. (a) Dose–response curves showing a dose-dependent decrease in metabolic activity in three different HNSCC cell lines in response to vactosertib. (b) Combination treatment of vactosertib with radiation showing significant differences on metabolic activity compared to single treatment. (c) Synergy maps showing a predominantly synergistic effect of vactosertib in combination with radiation for FaDu and SCC25, and an additive effect for SCC154 cell lines. (Calculations were made using synergyfinder.fimm.fi). (d) Trypan blue exclusion assay for effect of vactosertib on cell viability as single treatment and in combination with radiation. Significance levels were compared to the radiation dose-matched control. Graphs represent mean ± standard deviation. *p < 0.05, **p < 0.01, ***p < 0.001, and ****p < 0.0001.

at 8 Gy (ctrl.: 3.9% ± 3.8% vs. 75 μm: 18% ± 14.1%, $p < 0.001$), while SCC154 was unaffected by vactosertib treatment (Figure 3d right).

3.4 | Vactosertib reduces colony formation

To assess the inhibitory effect on clonogenic survival, colony formation assays were performed as described previously (Franken et al., 2006). FaDu and SCC25 showed a dose-dependent decrease in colony formation. In FaDu cells, vactosertib single treatment at 50 μM reduced the surviving fraction to 28% ± 19.6% ($p < 0.001$), which was further reduced in combination with 2 Gy radiation to 9.6% ± 10.4% ($p < 0.001$), (Figure 4a, top row). For SCC25, the vactosertib concentration was reduced due to a stronger inhibitory effect, which already showed inhibition to 13% ± 8.2% at 12.5 μm ($p < 0.001$) vactosertib single treatment. Combined with 2 Gy radiation, this was further reduced to 4.9% ± 3.7% ($p < 0.001$, Figure 4a middle row). In SCC154, vactosertib showed significant inhibition at 50 μM vactosertib single treatment to 41% ± 19% ($p < 0.001$). No additional effect in combination with radiation could be observed for this cell line (Figure 4a bottom).
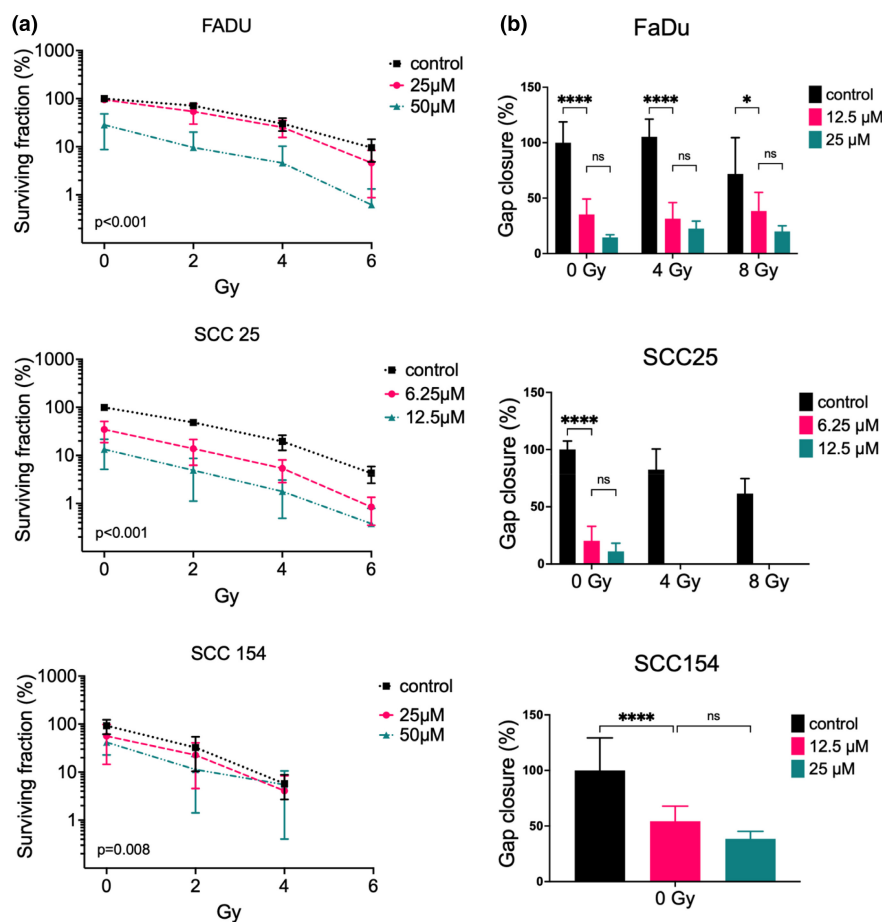
3.5 | Vactosertib inhibits cell migration

A migration assay was used to determine the effect of vactosertib on cell migration. Migration was significantly inhibited after vactosertib treatment in all three cell lines at low concentrations (Figure 4b). The strongest anti-migratory effect was observed in SCC25. At a concentration of 6.25 μM, we observed a reduction in gap closure of 80% in single treatment (ctrl.: 100% ± 7.5% vs. 6.25 μM: 20% ± 12.6%, $p < 0.001$). Combination with radiation led to an absolute inhibition of migration (Figure 4b, middle row). For SCC154, we also observed a significant inhibition at low-dose single treatment (ctrl: 100% ± 29% vs. 12.5 μM: 54% ± 13.5%, $p < 0.001$). Combination treatment was not feasible due to the high radiosensitivity of this cell line (Figure 4b, bottom row). FaDu showed the same significant effect at low concentration single treatment (ctrl: 100% ± 18% vs. 12.5 μM: 35% ± 13.9% $p < 0.001$); however, a combination with radiation led to no further inhibition (Figure 4b, top row).

3.6 | CAF-conditioned medium stimulates metabolic activity and cell migration which Vactosertib can abrogate

To investigate the effect of the tumor stroma on TGFBR1 inhibition in HNSCC cell lines, we performed indirect coculture experiments using a conditioned medium from patient-derived CAFs (CAF CM) of primary tumor samples. CAFs from three donors were included (Table S4). Metabolic activity was assessed using the resazurin assay described above. In FaDu, CAF CM#1 increased metabolic activity by 11% ± 15.9% ($p = 0.031$), while CAF CM#2 and 3 had no effect.

FIGURE 4 Effect of TGFBR1 inhibition on clonogenic survival and cell migration. (a) Survival curves derived from clonogenic assays in response to vactosertib treatment in combination with radiation. (b) Migration assay showing percentage of gap closure as a response to different treatment combinations. Combination treatment was not feasible for SCC154 because of the high radiosensitivity of this HPV⁺ cell line. Graphs report mean values ± standard deviation. *$p < 0.05$, **$p < 0.01$, ***$p < 0.001$, and ****$p < 0.0001$.

Treatment with 50 and 75 μM vactosertib abolished this stimulating effect (75 μM Vac.; ctrl.: 38% ± 10.5% vs. CAF CM#1: 37% ± 6.9%, $p = 0.994$; Figure 5a, left). SCC154 was the most sensitive cell line to CAF CM stimulation. CAF CM increased metabolic activity to between 138% ± 15.5% (CAF CM#2; $p < 0.001$) and 201% ± 26.5% (CAF CM#1; $p < 0.001$). Vactosertib treatment significantly inhibited this stimulating effect with increasing concentration (75 μM Vac.; ctrl.: 71% ± 18.7% vs. CAF CM#1: 81% ± 11.3%, $p = 0.957$, Figure 5a, right). SCC25, in contrast, showed no increase in metabolic activity after incubation with CAF CM. However, vactosertib treatment in combination with CAF CM increased metabolic activity at all concentrations (Figure 5a, middle). At 75 μM, CAF CM#2 and 3 still showed increased metabolic activity compared to the control (75 μM Vac.; ctrl: 24% ± 9% vs. CAF CM#2: 39.8% ± 8.3% vs. CAF CM#3: 39% ± 4.1%, $p < 0.001$, Figure 5a, middle).

Finally, we aimed to analyze the effect of CAF CM on cell migration. Migration assays were performed using CAF CM#1 since it showed the highest effect on metabolic activity. The incubation period was shortened to 14h for SCC25 and 18h for FaDu and SCC154 since gap closure was observed earlier in cells incubated with the CAF CM. Gap closure was normalized to untreated (0.1% DMSO control) and unstimulated (standard cell culture medium) control groups of each cell line. CAF CM#1 significantly increased gap closure in FaDu (ctrl.: 100% ± 11.7% vs. CAF CM#1: 141% ± 29%, $p < 0.000$) and SCC154 (ctrl.: 100% ± 30.6% vs. CAF CM#1: 170% ± 22.9%, $p < 0.001$). When cells were additionally treated with vactosertib, all three cell lines showed a significant decrease in cell migration compared to the CAF CM#1 group, with the strongest effect observed in FaDu (Figure 5b).

4 | DISCUSSION

In this study, we found that high TGFBR1 mRNA levels were independently associated with worse overall survival (OS) in HNSCC patients. At the protein level, we found a significant interaction between TGFBR1 expression in tumor cells and stromal cells. Patients who expressed TGFBR1 in tumor cells but were negative for TGFBR1 in stromal cells showed significantly poorer survival. In vitro experiments to evaluate the antineoplastic and radiosensitizing effect of a novel small molecule TGFBR1 inhibitor (vactosertib) on HPV[+] and HPV[−] HNSCC cell lines showed significant antineoplastic effects. Furthermore, we observed synergistic interactions of vactosertib with radiation, indicating its potential as a radiosensitizer. Finally, TGFBR1 inhibition could also largely abrogate the stimulatory effect of conditioned medium from patient-derived cancer-associated fibroblasts.

Radiation resistance remains a major cause of treatment failure in HNSCC patients. Radioresistance is a complex mechanism involving the tumor cells, tumor microenvironment, and immune cell response. To date, there are only two radiosensitizing drugs approved in HNSCC, namely cisplatin, a chemotherapeutic agent, and cetuximab, a monoclonal antibody against the epidermal growth factor receptor, which was approved in 2006 (Bernier et al., 2004; Labianca et al., 2007). However, a radiosensitizer that is highly effective and shows a low-toxicity profile at the same time is still not available.

Upregulation of the TGF-β pathway appears as a central mechanism in radioresistance with a wide range of downstream effects (Centurione & Aiello, 2016). Novel small molecule TGFBR1 inhibitors have already been developed and clinically evaluated in different malignancies (Wang et al., 2020). Since TGF-β is commonly increased in HNSCC (White et al., 2010), we hypothesize that TGF-ß receptor inhibition could also act as a radiosensitizer in HNSCC. However, data on the radiosensitizing effect of TGF-ß inhibition in HNSCC is sparse. Notably, our group recently investigated another TGFBR1 inhibitor, namely galunisertib, with high specificity to this receptor and found heterogeneous results with a radiosensitizing effect in only one of three tested HNSCC cell lines (Jank et al., 2022). We attributed those findings to the high specificity of the tested inhibitor to TGFBR1 together with known alterations of the TGF-ß pathway in the less responsive cell lines (Jank et al., 2022). In this study, we,

FIGURE 5 Effect of conditioned medium from patient-derived cancer-associated fibroblast. (a) Dose–response curves showing the effect of CAF conditioned medium and the inhibitory effect of vactosertib on metabolic activity. (b) Migration assay showing the effect of CAF CM#1 on cell migration and the inhibitory effect of vactosertib. Percentage gap closure shows the reduction of gap area normalized to the untreated control group. Graphs report mean value ± standard deviation. *$p < 0.05$, **$p < 0.01$, ***$p < 0.001$, and ****$p < 0.0001$.
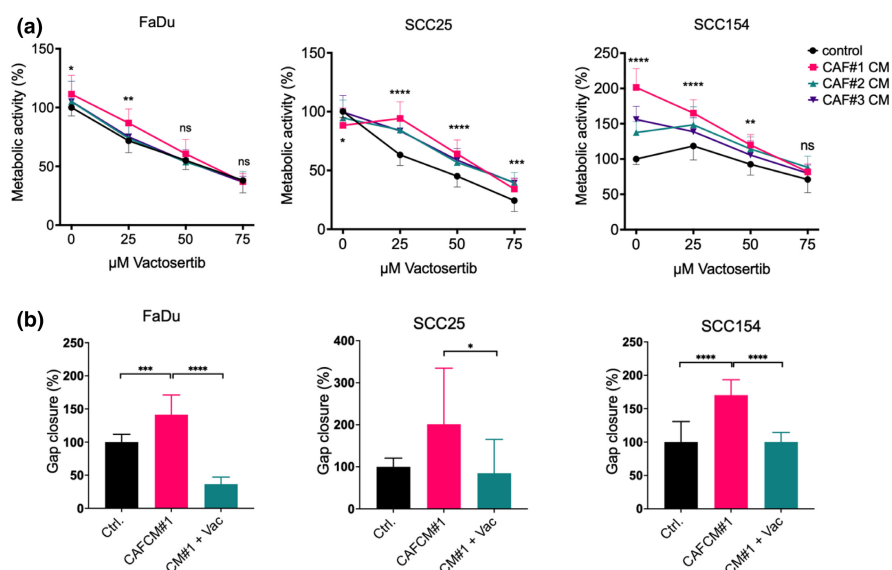
therefore, investigated an inhibitor with a broader mechanism of action against the TGF-ß signaling pathway. Furthermore, we aimed to investigate TGFBR1 protein expression in HNSCC and its association with survival.

We found that the majority of HNSCC patients were TGFBR1^{+}. We noticed distinct staining patterns between tumor cells and stromal cells and included this finding in our analysis based on the known dichotomous effect of TGF-ß signaling in cancer. Indeed, we found that TGFBR1+ primary tumors were associated with OS only in patients with TGFBR1- stroma. *Tumor*[TGFBR1+]|*stroma*[TGFBR1-] patients were almost five times more likely to die compared to *tumor*[TGFBR1+]|stroma[TGFBR1+] patients. This result might indicate a tumoristatic effect of TGFBR1 expression in the tumor stroma. In line with those results, we found that patients with TGFBR1+ staining in the stroma of lymph node metastasis showed significantly better OS compared to TGFBR1- patients. Patients with TGFBR1- stroma of lymph node metastasis showed particularly poor survival, with only a quarter of patients still alive after 5 years. Additionally, patients with TGFBR1- staining in tumor cells of lymph node metastasis showed excellent OS. This finding highlights the ambiguous role of TGF-ß signaling in malignant disease. While intact TGF-ß signaling acts as a tumor suppressor, altered signaling, usually occurring in more advanced stages of neoplastic disease, acts as a tumor promotor (Baba et al., 2022). Our results highlight that there is not only a temporal evolvement during disease progression but also spatial heterogeneity in TGF-ß function within the tumor and metastasis. While TGF-ß signaling in tumor cells of HNSCC is most likely corrupted and pro-oncogenic, stromal TGF-ß signaling within the tumor microenvironment might still exert antineoplastic effects. This finding might have important implications for future TGFBR1 inhibitor therapy. While TGFBR1 inhibition would appear reasonable in *tumor*[TGFBR1+]|*stroma*[TGFBR1-] HNSCC, it might be detrimental in *tumor*[TGFBR1-]|*stroma*[TGFBR1+] HNSCC. From a clinical perspective, evaluation of the TGFBR1 expression status by immunohistochemistry could easily be implemented into routine histopathological workup of tumor biopsies.

Although previous studies investigated TGFBR1 expression patterns in HNSCC, no study evaluated an interaction between the tumor cell and stromal staining or the association with disease outcome (Anderson et al., 1999; Eisma et al., 1996). However, Fanelli et al. investigated circulating tumor microemboli in patients with advanced HNSCC for TGFBR1 expression. They found that approximately one third was TGFBR1 positive, and this was associated with worse progression-free survival (Fanelli et al., 2017).

Noteworthy, we found an association between TGFBR1 expression and HPV status in both datasets, with HPV[−] patients showing a higher proportion of TGFBR1^{+} tumor cells. This difference might be explained by the fundamentally different molecular alterations in HPV[+] and HPV[−] HNSCC (Johnson et al., 2020). Indeed, Liu et al. (2018) could recently show that TGF-ß signaling is decreased in HPV[+] HNSCC using supervised clustering, and French et al. (2013) showed that the HPV16 oncoprotein E5 can downregulate TGFBR2. To exclude a confounding effect of HPV, we included HPV status

in the multivariable model, and no effect on disease outcome was observed between TGFBR1 and HPV (data not shown separately). To the best of our knowledge, this is the first report of TGFBR1 expression at different stages of disease progression and separated for tumor cell and stroma expression in HNSCC.

Finally, we evaluated the effect of vactosertib treatment in three HNSCC cell lines. Treatment decreased metabolic activity, a surrogate marker for cell viability, in a dose-dependent manner in all three cell lines. IC$_{50}$ values were observed in a clinically relevant range based on achievable plasma concentrations in a phase I study (Jung, Hwang, et al., 2020). Notably, combining vactosertib with radiation showed predominantly synergistic effects, especially in the HPV[−] HNSCC cell lines. The HPV[+] cell line also showed a synergistic effect at the clinically most relevant radiation dose of 2 Gy since radiation doses to HNSCC tumors are usually delivered at 2 Gy per session. The additional radiosensitizing effect might not be as pronounced in this cell line due to the inherently higher radiosensitivity (Arenz et al., 2014).

To date, no data exist on the radiosensitizing effect of vactosertib in HNSCC. In accordance with our results, treatment with other TGF-β inhibitors (LY364947, Galunisertib, and Fresolimumab) led to radiosensitization of HPV[−] HNSCC cell lines and marginal to no radiosensitization of HPV[+] cell lines (Liu et al., 2018). We observed a similar effect on clonogenic survival, which revealed a pronounced decrease in colony formation in FaDu and SCC25 but only a more subtle effect in SCC154. In contrast, the cytotoxic effect was minor, as determined by the trypan blue exclusion assay. Since vactosertib is not a cytotoxic drug, this can be expected at the tested concentrations. This circumstance may also be clinically advantageous due to the potentially less severe side effects of vactosertib compared to the currently used platinum-based radiosensitizers (cisplatin, carboplatin), which harbor considerable toxicity (Chow, 2020).

Cell migration is another important neoplastic mechanism controlled by TGF-ß signaling. Vactosertib significantly inhibited the migration of all HNSCC cell lines at low doses. SCC25 was sensitive to the extent that samples of combination treatment with radiation could not be evaluated due to the detachment of cells at the wound border. Also, in SCC154, a combination with radiation was not feasible due to the high radiosensitivity of this cell line. The strong anti-migratory effect of vactosertib has been previously described for other tumor entities like pancreatic cancer, prostate cancer, and breast cancer cells (Hong et al., 2020; Park et al., 2015; Son et al., 2014).

The tumor microenvironment, predominantly comprising CAFs, contributes to TGF-β secretion and plays a significant role in prognosis and tumor spread (Marsh et al., 2011; Peltanova et al., 2019; Wheeler et al., 2014). Indirect coculture experiments using CAF CM showed that the HPV[+] cell line was the most responsive. Notably, CAF CM#1 was also derived from an HPV[+] tumor, while CAF CM #2 and #3 were isolated from HPV[−] tumors. A potential effect of HPV status on TGF-ß levels was also suggested by a recent study, which showed that TGF-β levels were higher in the serum and saliva of patients with HPV[+] oropharyngeal tumors (OPSCC) compared to

HPV⁻ OPSCC (Polz-Dacewicz et al., 2016). Notably, this observation contrasts with a recent publication by Liu et al. (2018), which showed that HPV⁻ HNSCC cell lines responded stronger to TGF-ß stimulation than HPV⁺. However, our combined results indicate that TGF-β signaling also plays a significant role in HPV⁺ HNSCC.

Here, incubation of the HPV⁻ cell line FaDu with CAF CM showed a minor increase in cell viability, and this could be abrogated by vactosertib as expected. Interestingly, in SCC25, CAF CM showed no stimulatory effect. However, in combination with vactosertib, the metabolic activity significantly increased. A similar effect in SCC25 was observed in an earlier study by our group, as mentioned above. Paradoxically, treatment of SCC25 with galunisertib showed an increase in metabolic activity, while other neoplastic properties were inhibited (Jank et al., 2022). While we did not observe a similar effect for vactosertib treatment with the standard culture medium, this effect emerged in the CAF CM experiment. This observation might be explained by the difference in receptor specificity of both inhibitors. While galunisertib is highly selective to the TGFBR1, vactosertib also shows activity against ALK-5, another transmembrane receptor of the TGF-ß superfamily (Wang et al., 2020). Vactosertib treatment still led to a significant decrease in cell viability in a dose-dependent manner in all cell lines. These conflicting reports highlight that TGF-ß signaling is highly context-dependent, and many molecular mechanisms that control cellular processes remain largely elusive (Zhang et al., 2017). Also, the data on the role of TGF-ß signaling in combination with HPV status is still unclear in HNSCC and needs further research. Lastly, migration was also increased after incubation with CAF CM as expected based on previous work (Kumar et al., 2015; Peltanova et al., 2019; Wheeler et al., 2014), and vactosertib treatment abrogated this effect in all three cell lines.

There are five different limitations of this study that need to be discussed. First, TGFBR1 immunopathology analyses were performed by a single scientist (BJJ), albeit fully blinded to the dataset. Second, only one HPV⁺ cell line was used in this study, and our findings might not fully represent this disease entity. Third, the effect of CAFs on HNSCC cell lines was only observed in a one-way model via indirect coculture. However, a known interplay exists between HNSCC cells and CAFs (Wheeler et al., 2014). Fourth, cell death was analyzed using a trypan blue assay which does not specify the mechanism of cell death. Fifth, we did not evaluate the TGF-ß levels in CAF CM. Therefore, the observed differences cannot be attributed to this cytokine, although the stimulatory effect could be abrogated by a specific TGFBR1 inhibitor.

In this study, the comprehensive analysis of TGFBR1 expression in matched samples of HNSCC patients during disease progression and in vitro experiments revealed significant new findings on the potential of TGFBR1 as a drug target for radiosensitization. First, our data demonstrate distinct staining patterns of TGFBR1 expression between tumor cells and stromal cells, which bear significant prognostic value and might be useful as a predictive biomarker for TGFBR1-targeting agents. Second, vactosertib showed significant antineoplastic effects in all tested cell lines with a predominantly synergistic effect in combination with radiation, suggesting its potential as a radiosensitizer. Third, although HPV⁺ patients showed less frequent TGFBR1 expression, the HPV⁺ cell line significantly responded to TGBFR1 inhibition. Based on our findings, TGFBR1 is a promising candidate target for the radiosensitization of HNSCC and warrants further investigation to validate our results.

AUTHOR CONTRIBUTIONS

Bernhard J. Jank: Conceptualization; investigation; funding acquisition; writing – original draft; methodology; visualization; data curation; project administration. **Julia Schnoell:** Writing – original draft; investigation; methodology; visualization; formal analysis. **Katharina Kladnik:** Investigation; visualization; formal analysis; validation. **Carmen Sparr:** Investigation; methodology. **Markus Haas:** Investigation; methodology; visualization; formal analysis; software. **Elisabeth Gurnhofer:** Investigation; resources. **Alexander L. Lein:** Investigation; methodology. **Markus Brunner:** Conceptualization; methodology; supervision. **Lukas Kenner:** Conceptualization; resources; supervision; writing – review and editing. **Lorenz Kadletz-Wanke:** Investigation; methodology; writing – review and editing. **Gregor Heiduschka:** Conceptualization; methodology; resources; supervision.

CONFLICT OF INTEREST STATEMENT

No potential conflicts of interest were disclosed.

DATA AVAILABILITY STATEMENT

The data that support the findings of this study are available from the corresponding author upon reasonable request.

ETHICS STATEMENT

This study was approved by the ethics committee of the Medical University of Vienna (EK 2313/2019 and EK 1311/2018).

ORCID

Bernhard J. Jank https://orcid.org/0000-0003-1420-5034

REFERENCES

Anderson, M., Muro-Cacho, C., Cordero, J., Livingston, S., & Munoz-Antonia, T. (1999). Transforming growth factor beta receptors in verrucous and squamous cell carcinoma. *Archives of Otolaryngology – Head & Neck Surgery*, *125*(8), 849–854. https://doi.org/10.1001/archotol.125.8.849

Arenz, A., Ziemann, F., Mayer, C., Wittig, A., Dreffke, K., Preising, S., Wagner, S., Klussmann, J. P., Engenhart-Cabillic, R., & Wittekindt, C. (2014). Increased radiosensitivity of HPV-positive head and neck cancer cell lines due to cell cycle dysregulation and induction of apoptosis. *Strahlentherapie Und Onkologie*, *190*(9), 839–846. https://doi.org/10.1007/s00066-014-0605-5

Baba, A. B., Rah, B., Bhat, G. R., Mushtaq, I., Parveen, S., Hassan, R., Hameed Zargar, M., & Afroze, D. (2022). Transforming growth factor-Beta (TGF-beta) signaling in cancer-a betrayal within. *Frontiers in Pharmacology*, *13*, 791272. https://doi.org/10.3389/fphar.2022.791272

Bernier, J., Domenge, C., Ozsahin, M., Matuszewska, K., Lefèbvre, J. L., Greiner, R. H., Giralt, J., Maingon, P., Rolland, F., Bolla, M., Cognetti, F., Bourhis, J., Kirkpatrick, A., van Glabbeke, M., & European Organization for Research and Treatment of Cancer Trial 22931. (2004). Postoperative irradiation with or without concomitant chemotherapy for locally advanced head and neck cancer. *The New England Journal of Medicine*, 350(19), 1945–1952. https://doi.org/10.1056/NEJMoa032641

Bouquet, F., Pal, A., Pilones, K. A., Demaria, S., Hann, B., Akhurst, R. J., Babb, J. S., Lonning, S. M., DeWyngaert, J. K., Formenti, S. C., & Barcellos-Hoff, M. H. (2011). TGFbeta1 inhibition increases the radiosensitivity of breast cancer cells in vitro and promotes tumor control by radiation in vivo. *Clinical Cancer Research*, 17(21), 6754–6765. https://doi.org/10.1158/1078-0432.CCR-11-0544

Centurione, L., & Aiello, F. B. (2016). DNA repair and cytokines: TGF-beta, IL-6, and thrombopoietin as different biomarkers of Radioresistance. *Frontiers in Oncology*, 6, 175. https://doi.org/10.3389/fonc.2016.00175

Cerami, E., Gao, J., Dogrusoz, U., Gross, B. E., Sumer, S. O., Aksoy, B. A., Jacobsen, A., Byrne, C. J., Heuer, M. L., Larsson, E., Antipin, Y., Reva, B., Goldberg, A. P., Sander, C., & Schultz, N. (2012). The cBio cancer genomics portal: An open platform for exploring multidimensional cancer genomics data. *Cancer Discovery*, 2(5), 401–404. https://doi.org/10.1158/2159-8290.CD-12-0095

Chaturvedi, A. K., Engels, E. A., Pfeiffer, R. M., Hernandez, B. Y., Xiao, W., Kim, E., Jiang, B., Goodman, M. T., Sibug-Saber, M., Cozen, W., Liu, L., Lynch, C. F., Wentzensen, N., Jordan, R. C., Altekruse, S., Anderson, W. F., Rosenberg, P. S., & Gillison, M. L. (2011). Human papillomavirus and rising oropharyngeal cancer incidence in the United States. *Journal of Clinical Oncology*, 29(32), 4294–4301. https://doi.org/10.1200/JCO.2011.36.4596

Chow, L. Q. M. (2020). Head and neck cancer. *The New England Journal of Medicine*, 382(1), 60–72. https://doi.org/10.1056/NEJMra1715715

Eisma, R. J., Spiro, J. D., von Biberstein, S. E., Lindquist, R., & Kreutzer, D. L. (1996). Decreased expression of transforming growth factor beta receptors on head and neck squamous cell carcinoma tumor cells. *American Journal of Surgery*, 172(6), 641–645. https://doi.org/10.1016/s0002-9610(96)00305-4

Erdogan, B., & Webb, D. J. (2017). Cancer-associated fibroblasts modulate growth factor signaling and extracellular matrix remodeling to regulate tumor metastasis. *Biochemical Society Transactions*, 45(1), 229–236. https://doi.org/10.1042/BST20160387

Fanelli, M. F., Oliveira, T. B., Braun, A. C., Corassa, M., Abdallah, E. A., Nicolau, U. R., da Silva Alves, V., Garcia, D., Calsavara, V. F., Kowalski, L. P., & Chinen, L. T. D. (2017). Evaluation of incidence, significance, and prognostic role of circulating tumor microemboli and transforming growth factor-beta receptor I in head and neck cancer. *Head & Neck*, 39(11), 2283–2292. https://doi.org/10.1002/hed.24899

Franken, N. A., Rodermond, H. M., Stap, J., Haveman, J., & van Bree, C. (2006). Clonogenic assay of cells in vitro. *Nature Protocols*, 1(5), 2315–2319. https://doi.org/10.1038/nprot.2006.339

French, D., Belleudi, F., Mauro, M. V., Mazzetta, F., Raffa, S., Fabiano, V., Frega, A., & Torrisi, M. R. (2013). Expression of HPV16 E5 down-modulates the TGFbeta signaling pathway. *Molecular Cancer*, 12, 38. https://doi.org/10.1186/1476-4598-12-38

Gao, J., Aksoy, B. A., Dogrusoz, U., Dresdner, G., Gross, B., Sumer, S. O., Sun, Y., Jacobsen, A., Sinha, R., Larsson, E., Cerami, E., Sander, C., & Schultz, N. (2013). Integrative analysis of complex cancer genomics and clinical profiles using the cBioPortal. *Science Signaling*, 6(269), pl1. https://doi.org/10.1126/scisignal.2004088

Hong, E., Park, S., Ooshima, A., Hong, C. P., Park, J., Heo, J. S., Lee, S., An, H., Kang, J. M., Park, S. H., Park, J. O., & Kim, S. J. (2020). Inhibition of TGF-beta signalling in combination with nal-IRI plus 5-fluorouracil/leucovorin suppresses invasion and prolongs survival in pancreatic

tumour mouse models. *Scientific Reports*, 10(1), 2935. https://doi.org/10.1038/s41598-020-59893-5

Ianevski, A., He, L., Aittokallio, T., & Tang, J. (2020). SynergyFinder: A web application for analyzing drug combination dose-response matrix data. *Bioinformatics*, 36(8), 2645. https://doi.org/10.1093/bioinformatics/btaa102

Jank, B. J., Haas, M., Schnoell, J., Schlederer, M., Heiduschka, G., Kenner, L., & Kadletz-Wanke, L. (2021). Micro-crystallin is associated with disease outcome in head and neck squamous cell carcinoma. *Journal of Personalized Medicine*, 11(12), 1330. https://doi.org/10.3390/jpm11121330

Jank, B. J., Lenz, T., Haas, M., Kadletz-Wanke, L., Campion, N. J., Schnoell, J., Heiduschka, G., & Macfelda, K. (2022). Radiosensitizing effect of galunisertib, a TGF-ss receptor I inhibitor, on head and neck squamous cell carcinoma in vitro. *Investigational New Drugs*, 40(3), 478–486. https://doi.org/10.1007/s10637-021-01207-1

Johnson, D. E., Burtness, B., Leemans, C. R., Lui, V. W. Y., Bauman, J. E., & Grandis, J. R. (2020). Head and neck squamous cell carcinoma. *Nature Reviews. Disease Primers*, 6(1), 92. https://doi.org/10.1038/s41572-020-00224-3

Jung, S. Y., Hwang, S., Clarke, J. M., Bauer, T. M., Keedy, V. L., Lee, H., Park, N., Kim, S. J., & Lee, J. I. (2020). Pharmacokinetic characteristics of vactosertib, a new activin receptor-like kinase 5 inhibitor, in patients with advanced solid tumors in a first-in-human phase 1 study. *Investigational New Drugs*, 38(3), 812–820. https://doi.org/10.1007/s10637-019-00835-y

Jung, S. Y., Yug, J. S., Clarke, J. M., Bauer, T. M., Keedy, V. L., Hwang, S., Kim, S. J., Chung, E. K., & Lee, J. I. (2020). Population pharmacokinetics of vactosertib, a new TGF-beta receptor type iota inhibitor, in patients with advanced solid tumors. *Cancer Chemotherapy and Pharmacology*, 85(1), 173–183. https://doi.org/10.1007/s00280-019-03979-z

Kaowinn, S., Kim, J., Lee, J., Shin, D. H., Kang, C. D., Kim, D. K., Lee, S., Kang, M. K., Koh, S. S., Kim, S. J., & Chung, Y. H. (2017). Cancer upregulated gene 2 induces epithelial-mesenchymal transition of human lung cancer cells via TGF-beta signaling. *Oncotarget*, 8(3), 5092–5110. https://doi.org/10.18632/oncotarget.13867

Kumar, D., Kandl, C., Hamilton, C. D., Shnayder, Y., Tsue, T. T., Kakarala, K., Ledgerwood, L., Sun, X. S., Huang, H. J., Girod, D., & Thomas, S. M. (2015). Mitigation of tumor-associated fibroblast-facilitated head and neck cancer progression with anti-hepatocyte growth factor antibody Ficlatuzumab. *JAMA Otolaryngology. Head & Neck Surgery*, 141(12), 1133–1139. https://doi.org/10.1001/jamaoto.2015.2381

Labianca, R., La Verde, N., & Garassino, M. C. (2007). Development and clinical indications of cetuximab. *The International Journal of Biological Markers*, 22(1 Suppl 4), S40–S46.

Liu, Q., Ma, L., Jones, T., Palomero, L., Pujana, M. A., Martinez-Ruiz, H., Ha, P. K., Murnane, J., Cuartas, I., Seoane, J., Baumann, M., Linge, A., & Barcellos-Hoff, M. H. (2018). Subjugation of TGFbeta signaling by human papilloma virus in head and neck squamous cell carcinoma shifts DNA repair from homologous recombination to alternative end joining. *Clinical Cancer Research*, 24(23), 6001–6014. https://doi.org/10.1158/1078-0432.CCR-18-1346

Marsh, D., Suchak, K., Moutasim, K. A., Vallath, S., Hopper, C., Jerjes, W., Upile, T., Kalavrezos, N., Violette, S. M., Weinreb, P. H., Chester, K. A., Chana, J. S., Marshall, J. F., Hart, I. R., Hackshaw, A. K., Piper, K., & Thomas, G. J. (2011). Stromal features are predictive of disease mortality in oral cancer patients. *The Journal of Pathology*, 223(4), 470–481. https://doi.org/10.1002/path.2830

Park, S. A., Kim, M. J., Park, S. Y., Kim, J. S., Lee, S. J., Woo, H. A., Kim, D. K., Nam, J. S., & Sheen, Y. Y. (2015). EW-7197 inhibits hepatic, renal, and pulmonary fibrosis by blocking TGF-beta/Smad and ROS signaling. *Cellular and Molecular Life Sciences*, 72(10), 2023–2039. https://doi.org/10.1007/s00018-014-1798-6

Peltanova, B., Raudenska, M., & Masarik, M. (2019). Effect of tumor microenvironment on pathogenesis of the head and neck squamous

cell carcinoma: A systematic review. *Molecular Cancer*, 18(1), 63. https://doi.org/10.1186/s12943-019-0983-5

Perri, F., Pacelli, R., Della Vittoria Scarpati, G., Cella, L., Giuliano, M., Caponigro, F., & Pepe, S. (2015). Radioresistance in head and neck squamous cell carcinoma: Biological bases and therapeutic implications. *Head & Neck*, 37(5), 763–770. https://doi.org/10.1002/hed.23837

Polz-Dacewicz, M., Strycharz-Dudziak, M., Dworzanski, J., Stec, A., & Kocot, J. (2016). Salivary and serum IL-10, TNF-alpha, TGF-beta, VEGF levels in oropharyngeal squamous cell carcinoma and correlation with HPV and EBV infections. *Infectious Agents and Cancer*, 11, 45. https://doi.org/10.1186/s13027-016-0093-6

Sheen, Y. Y., Kim, M. J., Park, S. A., Park, S. Y., & Nam, J. S. (2013). Targeting the transforming growth factor-beta signaling in cancer therapy. *Biomolecules & Therapeutics*, 21(5), 323–331. https://doi.org/10.4062/biomolther.2013.072

Son, J. Y., Park, S. Y., Kim, S. J., Lee, S. J., Park, S. A., Kim, M. J., Kim, S. W., Kim, D. K., Nam, J. S., & Sheen, Y. Y. (2014). EW-7197, a novel ALK-5 kinase inhibitor, potently inhibits breast to lung metastasis. *Molecular Cancer Therapeutics*, 13(7), 1704–1716. https://doi.org/10.1158/1535-7163.MCT-13-0903

Song, K. M., Chung, D. Y., Choi, M. J., Ghatak, K., Minh, N. N., Limanjaya, A., Kwon, M. H., Ock, J., Yin, G. N., Kim, D. K., Ryu, J. K., & Suh, J. K. (2019). Vactosertib, a novel, orally bioavailable activin receptor-like kinase 5 inhibitor, promotes regression of fibrotic plaques in a rat model of Peyronie's disease. *The World Journal of Men's Health*, 38, 552–563. https://doi.org/10.5534/wjmh.190071

Sung, H., Ferlay, J., Siegel, R. L., Laversanne, M., Soerjomataram, I., Jemal, A., & Bray, F. (2021). Global cancer statistics 2020: GLOBOCAN estimates of incidence and mortality worldwide for 36 cancers in 185 countries. *CA: A Cancer Journal for Clinicians*, 71(3), 209–249. https://doi.org/10.3322/caac.21660

Teicher, B. A. (2021). TGFbeta-directed therapeutics: 2020. *Pharmacology & Therapeutics*, 217, 107666. https://doi.org/10.1016/j.pharmthera.2020.107666

Tian, M., & Schiemann, W. P. (2009). The TGF-beta paradox in human cancer: An update. *Future Oncology*, 5(2), 259–271. https://doi.org/10.2217/14796694.5.2.259

Wang, H., Chen, M., Sang, X., You, X., Wang, Y., Paterson, I. C., Hong, W., & Yang, X. (2020). Development of small molecule inhibitors targeting TGF-beta ligand and receptor: Structures, mechanism, preclinical studies and clinical usage. *European Journal of Medicinal Chemistry*, 191, 112154. https://doi.org/10.1016/j.ejmech.2020.112154

Wheeler, S. E., Shi, H., Lin, F., Dasari, S., Bednash, J., Thorne, S., Watkins, S., Joshi, R., & Thomas, S. M. (2014). Enhancement of head and neck squamous cell carcinoma proliferation, invasion, and metastasis by tumor-associated fibroblasts in preclinical models. *Head & Neck*, 36(3), 385–392. https://doi.org/10.1002/hed.23312

White, R. A., Malkoski, S. P., & Wang, X. J. (2010). TGFbeta signaling in head and neck squamous cell carcinoma. *Oncogene*, 29(40), 5437–5446. https://doi.org/10.1038/onc.2010.306

Yamamoto, V. N., Thylur, D. S., Bauschard, M., Schmale, I., & Sinha, U. K. (2016). Overcoming radioresistance in head and neck squamous cell carcinoma. *Oral Oncology*, 63, 44–51. https://doi.org/10.1016/j.oraloncology.2016.11.002

Yoon, J. H., Jung, S. M., Park, S. H., Kato, M., Yamashita, T., Lee, I. K., Sudo, K., Nakae, S., Han, J. S., Kim, O. H., Oh, B. C., Sumida, T., Kuroda, M., Ju, J. H., Jung, K. C., Park, S. H., Kim, D. K., & Mamura, M. (2013). Activin receptor-like kinase5 inhibition suppresses mouse melanoma by ubiquitin degradation of Smad4, thereby derepressing eomesodermin in cytotoxic T lymphocytes. *EMBO Molecular Medicine*, 5(11), 1720–1739. https://doi.org/10.1002/emmm.201302524

Yu, Y., Xiao, C. H., Tan, L. D., Wang, Q. S., Li, X. Q., & Feng, Y. M. (2014). Cancer-associated fibroblasts induce epithelial-mesenchymal transition of breast cancer cells through paracrine TGF-beta signalling. *British Journal of Cancer*, 110(3), 724–732. https://doi.org/10.1038/bjc.2013.768

Zhang, Y., Alexander, P. B., & Wang, X. F. (2017). TGF-beta family signaling in the control of cell proliferation and survival. *Cold Spring Harbor Perspectives in Biology*, 9(4), a022145. https://doi.org/10.1101/cshperspect.a022145

SUPPORTING INFORMATION

Additional supporting information can be found online in the Supporting Information section at the end of this article.